Shear in Discontinuity Regions

Changes for the ACI 318 Building Code

by Gary J. Klein, Nazanin Rezaei, David Garber, and A. Koray Tureyen

The strut-and-tie method was introduced into "Building Code Requirements for Structural Concrete" (ACI 318) in 2002,[1] although its origins date to the end of the nineteenth century.[1] The ACI 318-02 version of the strut-and-tie method is largely based on a 1987 report by Schlaich et al.[2] that describes procedures for designing structural elements using a system of struts and ties connected at nodes. The method is primarily intended for regions of the structure where the stress flow is influenced by concentrated loads, corners, openings, or other discontinuities. Such regions are referred to as discontinuity regions or D-regions. Strain distribution in D-regions is highly nonlinear, and the assumption of plane sections remaining plane does not apply. The strut-and-tie method is especially useful in D-regions because it allows for designing and detailing of the concrete section and reinforcement in accordance with a clearly visualized force field that is in static equilibrium, rather than relying on past practices or restrictive empirical guidelines.

However, as will be explained in this article, there are several concerns and inconsistencies in the current Code (ACI 318-14[3]) related to shear strength in D-regions:

- Except for members qualifying as deep beams, minimum distributed reinforcement is not required in a D-region designed by the strut-and-tie method;
- Interior struts (struts not located along a boundary of a D-region) are not weaker than boundary struts because they are "bottle-shaped"; rather, the apparent weakness arises because interior struts cross a diagonal tension field;
- The strut efficiency factor β_s for interior struts is unconservative because D-regions can fail in shear, which is not considered in the strut-and-tie method;
- According to the Code Commentary, the shear stress in deep beams is limited to control cracking. The limiting stress is $10A_{cv}\sqrt{f_c'}$, where f_c' is the specified compressive strength of the concrete in psi ($\sqrt{\text{psi}}$ units are used herein; $1\sqrt{\text{psi}} = 0.083\sqrt{\text{MPa}}$). This limit does not apply to members or D-regions that do not "qualify" as deep beams, which is inconsistent at best. Furthermore, this limit is unnecessarily restrictive for D-regions with steeply inclined interior struts;
- Size effect λ_s is not considered; and
- The lightweight concrete factor λ is used as a multiplier on f_c' rather than on $\sqrt{f_c'}$, as it is elsewhere in the Code.

This article describes the rationale for Code changes that will be in ACI 318-19 (scheduled for publication in June 2019) that address these concerns and inconsistencies while maintaining the essential characteristics of design according to the strut-and-tie method. The Code changes relate to the strength of struts and requirements for minimum distributed reinforcement. The changes are based on review of relevant literature, analysis of published test data, and an experimental program designed to evaluate the influence of diagonal tension on the strength of struts.

Strength of Struts

Bottle-shaped struts

ACI 318-14 defines a bottle-shaped strut as a strut that is wider at mid-length than at its ends. The Code also specifies a strut efficiency factor β_s of 0.6 for unreinforced bottle-shaped struts and $\beta_s = 0.75$ for reinforced bottle-shaped struts. However, research and testing by Laughery and Pujol[4] shows that bottle-shaped struts are no weaker than prismatic struts. Referring to Fig. 1, prismatic (a) and two-dimensional (2-D) bottle-shaped struts (b) exhibited approximately equal strength, both averaging about 0.85 f_c', which is equivalent to a β_s of 1.0. Prismatic and 2-D bottle-shaped struts were less than half as strong as three-dimensional (3-D) bottle-shaped struts (Fig. 1(c)).

In an element like that shown in Fig. 1(b), stresses spread laterally between the concentrated load or reaction areas and mid-length of the strut without the presence of a diagonal tension field. However, in deep beams and other D-regions, the stress flow is much more complex. As illustrated in Fig. 2, struts between the load and reaction in a deep beam cross through a field of diagonal tension. For the model shown in Fig. 2, the strut is inclined at about 55 degrees and the diagonal tensile stress at mid-depth is 66% of that calculated assuming plane sections remain plane. For the same shear force, diagonal tensile stress at mid-depth decreases as the strut angle increases. When the strut is vertical, like the element shown in Fig. 1(b), the bursting stress at mid-height due to bottle-shaped behavior is much smaller than the diagonal tensile stress across inclined struts.

These observations indicate that the strength of deep beams and other D-regions is limited by diagonal tension rather than splitting due to bottle-shaped stress flow. For this reason, ACI 318-19 will not use the term *bottle-shaped* struts. Struts that extend diagonally through the interior of D-regions will be defined as *interior* struts. Struts that carry compressive force along a boundary of a D-region will be defined as *boundary* struts.

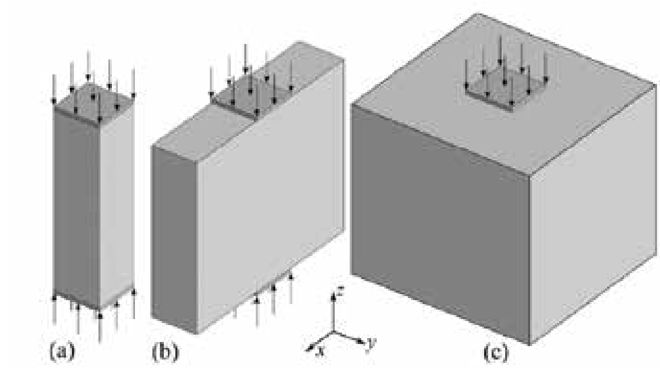

Fig. 1: Illustrations of: (a) rectangular prismatic strut; (b) 2-D rectangular bottle-shaped strut; and (c) 3-D rectangular bottle-shaped strut (after Laughery and Pujol[4])

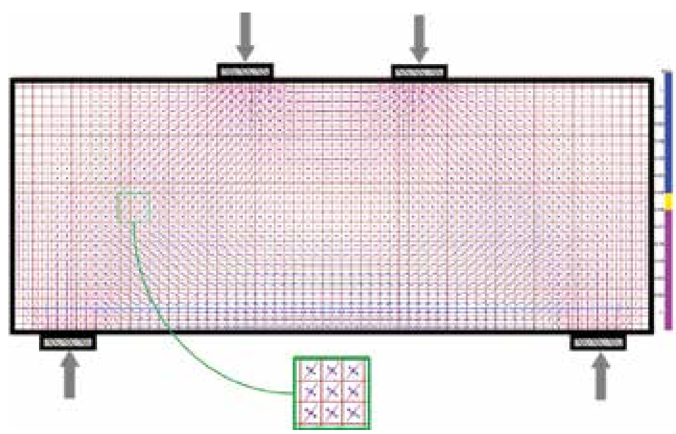

Fig. 2: Example of stress flow in a deep beam. Blue lines in the inset indicate tension orientation

Unreinforced struts

Reineck and Todisco[5] evaluated the strut strength coefficients β_s in ACI 318-14 relative to test data in the ACI-DAfStb Database[6] for members without transverse reinforcement. The database variables include shear span a_v, specimen width b, and distance d from the extreme compression fiber to centroid of longitudinal tension reinforcement. Measured shear strength V_{test} was compared to the shear strength calculated in accordance with the strut-and-tie method in ACI 318-14, V_{calc}. Several test values were much less than predicted by ACI 318-14 methods throughout the full range of a_v/d considered. Based on these findings, Reineck and Todisco[5] recommended that β_s be reduced from 0.6 to 0.42.

The findings are shown in Fig. 3 as a plot of V_{test}/V_{calc} versus f_c'. In this plot, the calculated shear strength was based on Reineck and Todisco Alternative 3, in which the depth of the compression zone c was calculated for the load at shear failure.[5] The trendline indicates that V_{test}/V_{calc} decreases with increasing f_c'. For the higher concrete strengths, the trendline closely follows $100\sqrt{f_c'}/f_c'$ (the solid gray line), which is the expected trendline for failures that are proportional to $\sqrt{f_c'}$ rather than f_c'. This observation strongly indicates that most failures in the joint ACI-DAfStb Database[6] are due to diagonal tension (which varies with $\sqrt{f_c'}$) rather than splitting due to strut compression. This finding is consistent with the failure descriptions in the database and research papers from which the database was developed.

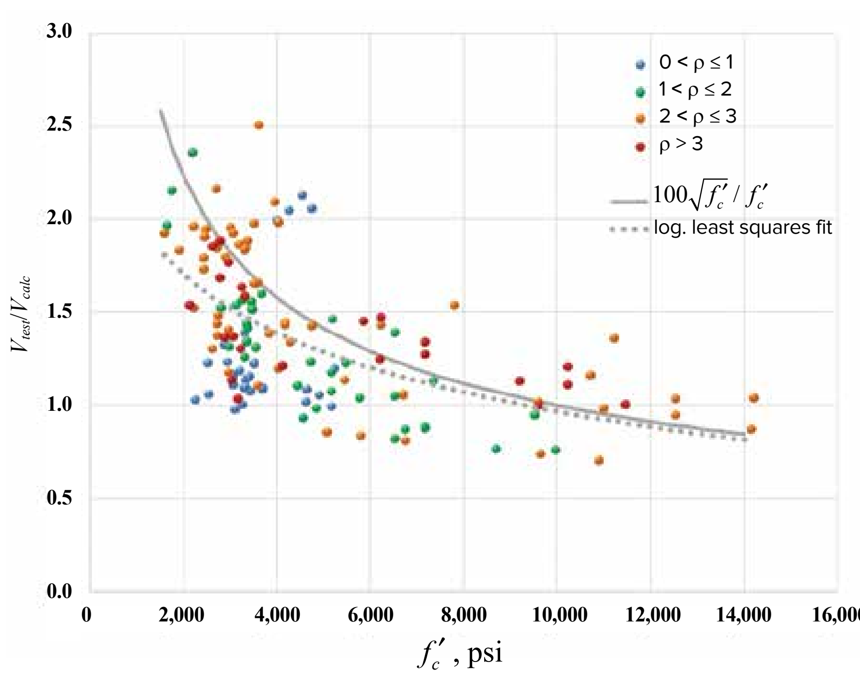

Fig. 3: V_{test}/V_{calc} versus f_c' (Note: V_{calc} in accordance with the strut-and-tie method in ACI 318-14; ρ = longitudinal reinforcement ratio, %)

Table 1:
Specimen details and test results

Specimen		Dimensions, in. (mm)			Strut angle, deg.	f_c', ksi (MPa)	Failure load, kip (kN)	β_s	$\frac{\text{Truss}}{\text{Rect.}}$
Name	Type	Height	Length	Thickness					
Re-30-Ex	Rect.	31.3 (795)	96 (2438)	12 (305)	30	7.44 (51.3)	380 (1960)	0.43	1.51
Tr-30-Ex	Truss	31.3 (795)	96 (2438)	12 (305)	30	7.37 (50.8)	575 (2558)	0.66	
Re-45-Ex	Rect.	48 (1219)	96 (2438)	12 (305)	45	5.63 (38.8)	557 (2478)	0.58	1.29
Tr-45-Ex	Truss	48 (1219)	96 (2438)	12 (305)	45	5.63 (38.8)	717 (3189)	0.74	

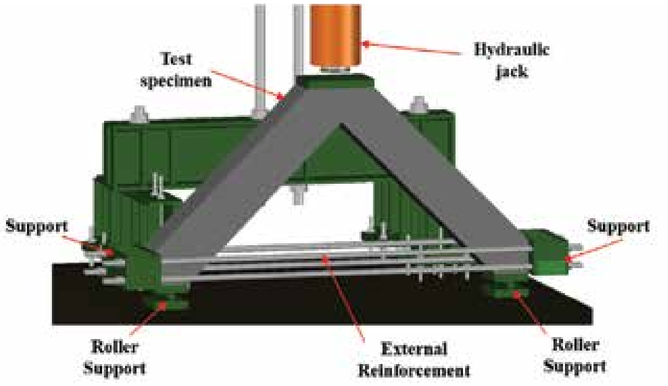

Fig. 4: Schematic of test setup and specimen with supports (truss-like specimen shown)

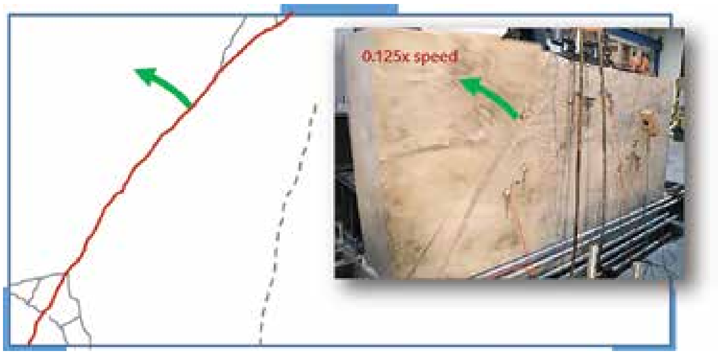

Fig. 5: Failure crack pattern and image of instant of failure for specimen Re-45-Ex

Experimental study

An experimental study was conducted at Florida International University to investigate the behavior of struts in deep beams without distributed reinforcement. The full experimental study involved the testing of 10 full-scale specimens as described in a companion paper[7]; the results from four of these specimens are discussed herein (refer to Table 1).

Two pairs of rectangular and truss-like specimens were tested using the setup shown in Fig. 4. The first pair consisted of a rectangular specimen and a truss-like specimen with identical overall dimensions and similar concrete compressive strengths. The height of the specimens was selected such that the strut angle was 30 degrees from horizontal. The height of the second pair was increased such that the strut angle was 45 degrees, and the concrete compressive strength somewhat lower than that of the first pair.

The shape of the truss-like specimens (Fig. 4) precluded development of diagonal tension across the strut. Comparison of the truss-like specimens to their rectangular counterparts allows for evaluation of the effect of diagonal tension on strut strength.

The specimens were tested to failure. The rectangular specimens failed in diagonal tension, while the truss-like specimens failed primarily by crushing of the concrete. All specimens failed suddenly and violently. The cracking pattern for specimen Re-45-Ex is shown in Fig. 5. The instant of failure captured from slow-motion video is shown in the inset image. The primary failure crack (red line) appears to initiate at the curved green arrow. Additional secondary cracks developed due to restraint at the load and reaction areas as the upper corner of the specimen rotated away about the support, as indicated by the green arrow. The estimated pattern of secondary cracks is illustrated in gray lines in Fig. 5. The other rectangular beam specimen, Re-30-Ex, failed in a similar fashion.

The truss-like specimens failed primarily by crushing of the concrete just below the load area. As load was applied, the struts shortened, and the reaction points separated, adding bending stress to the strut compressive stress. Therefore, the strut strength factors β_s for the truss-like specimens were about 0.75.

The truss-like specimens with 30- and 45-degree strut angles were about 50 and 30% stronger than their rectangular counterparts, respectively. As discussed by Van den Hoogen,[8] Beeby observed a comparable difference between a rectangular specimen and a similar specimen that included a triangular cutout at the bottom of the specimen. Considering the previously discussed Laughery and Pujol findings,[4] the reduced strength of rectangular specimens appears to be due to diagonal tension rather than a bottle-shaped stress field.

Shear Strength of D-Regions

The research described previously indicates D-regions usually fail in shear before the strut crushes. This section explores the factors that influence shear strength of D-regions.

Strut angle

Consider the full-story transfer girder illustrated in Fig. 6 and the shear stresses along line a-a. Such a girder might be used at an offset in the column grid. The shear force is carried by a direct strut between the bottom of the top column and top of the bottom column. In taller buildings, shear stresses can substantially exceed the $10\sqrt{f_c'}$ limit in ACI 318-14.

Zsutty[9] reported on the inverse relationship between shear strength and a_v/d. He recommended a multiplier of $2.5/(a_v/d)$ to account for the effect of shear span. This expression times $2\sqrt{f_c'}b_w d$ gives the following expression for shear strength of D-regions

$$V_c = \frac{5\sqrt{f_c'}b_w d}{(a_v/d)} \quad (1)$$

ACI 318-19 will consider shear force based on strut angle θ, where tan θ is substituted for $1/(a_v/d)$ in Eq. (1) to give the following equation

$$V_u \leq \phi 5 \tan\theta \sqrt{f_c'}b_w d \quad (1a)$$

Figure 7 is a plot of shear stress at failure versus a_v/d. The data are from the joint ACI-DAfStb Database[6] for members without transverse reinforcement and a_v/d of 2.0 or less. At very low a_v/d, the shear strength substantially exceeds the shear stress limit of $10\sqrt{f_c'}$ specified in the Code. The shallowest allowable strut angle of 25 degrees corresponds to an a_v/d of about 2 and a shear stress limit of $2.5\sqrt{f_c'}$. The gray line shows the shear stress given by Eq. (1) expressed in terms of $\sqrt{f_c'}$. All data points are near or above the line, indicating that Eq. (1) provides a conservative lower bound to the shear strength of D-regions in the joint ACI-DAfStb Database,[6] even if strut compression is controlled. As would be expected, the lower values correspond to members with low ratios of longitudinal reinforcement.

Size effect and lightweight concrete factors

Equation (1) does not include reductions in shear strength due to size effect or reduced mechanical properties of lightweight concrete, although both factors would be expected to reduce shear strength as governed by diagonal tension. However, these factors are not especially important for the comparison shown in Fig. 7, because the joint ACI-DAfStb Database[6] primarily includes relatively small specimens fabricated with normalweight concrete.

For more than 30 years, researchers have recognized that size effect can significantly reduce the shear strength of deep members without transverse reinforcement, such as footings and thick one-way slabs.[10] ACI 318-19 sectional design equations for both one-way and two-way shear strength will include a size effect factor[11] λ_s:

$$\lambda_s = \sqrt{\frac{2}{1+d/10}} \leq 1.0$$

where d is in in. (the SI equivalent is $\sqrt{2/(1+d/254)}$, where d is in mm).

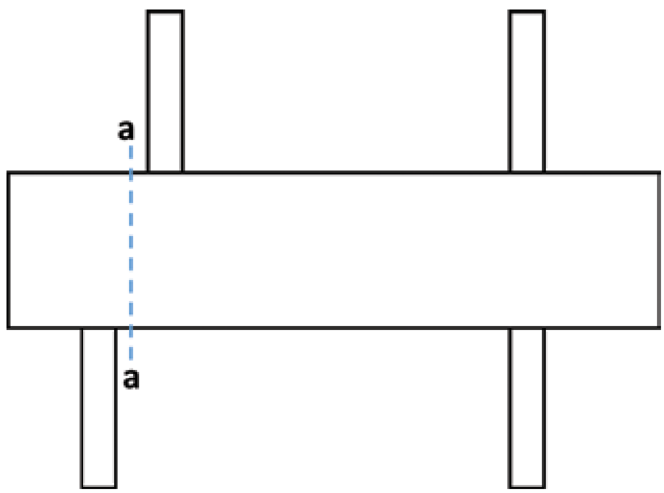

Fig. 6: Transfer girder at an offset in the column grid

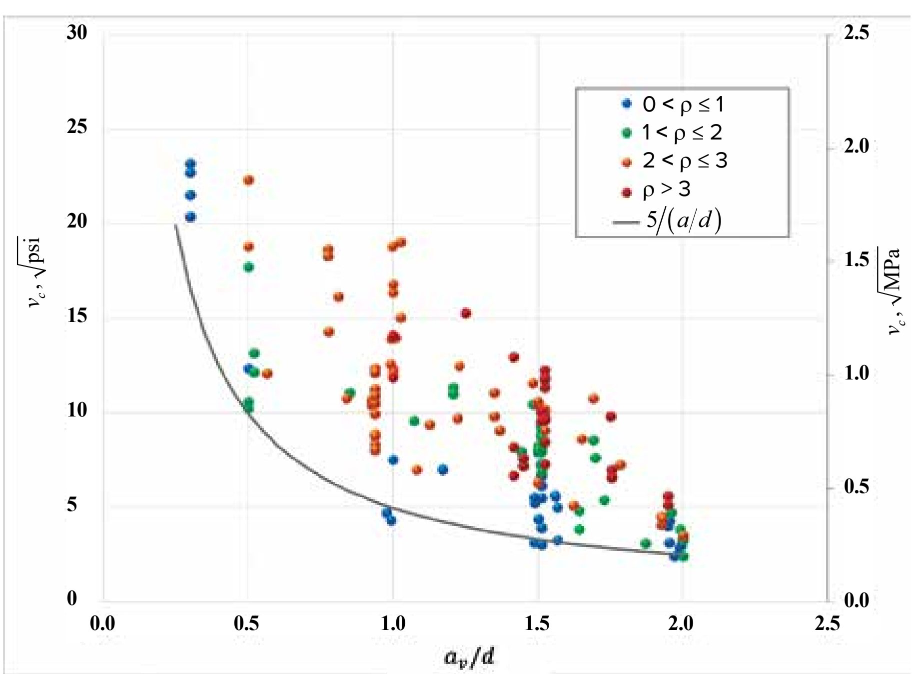

Fig. 7: Shear stress v_c versus ratio of shear span to effective depth, a_v/d (Note: $v_c = V_{test}/bd$)

Also, because the basis of the proposed design equation is diagonal tension, the lightweight concrete factor λ should be considered to account for the lower tensile-compressive strength ratio of lightweight concrete compared with normalweight concrete.

Including size effect and the reduced tensile-compressive strength properties of lightweight concrete, Eq. (1a) becomes

$$V_c = \phi 5 \lambda \lambda_s \tan\theta \sqrt{f_c'} b_w d \quad (2)$$

Distributed reinforcement

The strut-and-tie method is derived from the lower-bound theorem of plasticity. Distributed reinforcement in discontinuity regions helps redistribute internal forces, which is especially important where the assumed strut-and-tie model is not entirely consistent with the flow of internal stresses. In addition to allowing force redistribution, distributed reinforcement controls cracking at service loads and promotes ductile behavior. Analysis of the joint ACI-DAfStb Database[6] for members with a distributed reinforcement ratio of at least 0.25% indicates the current β_s value of 0.75 is safe such that an independent check of shear strength of the section is not required. However, we recommend verifying diagonal tension strength using Eq. (2) in regions where struts connect to hanger reinforcement, such as the nibs of dapped-end connections, even if distributed reinforcement is provided. Testing sponsored by PCI[12] indicates such regions are vulnerable to diagonal tension failure due to tensile stress induced by the hanger reinforcement, despite distributed horizontal reinforcement.

Code Changes for ACI 318-19

Based on these findings, several changes to the ACI Code were approved by ACI Committee 318:

- Struts that extend diagonally through the interior of D-regions will be defined as interior struts rather than bottle-shaped struts. Struts that carry compressive force along a boundary of a D-region will be defined as boundary struts;
- Distributed reinforcement will be required in all discontinuity regions unless the strut is laterally confined. The minimum effective reinforcement ratio is 0.25%. The lateral confinement exception applies to members like pile caps and continuous beam ledges, where distributed reinforcement is unnecessary and impractical. If distributed reinforcement is provided, the strut efficiency factor β_s may be taken as 0.75;
- For members without transverse reinforcement, an independent check of shear stress in accordance with Eq. (2) will be required unless β_s is taken as 0.4. Equation (2) accounts for both size effect and the reduced mechanical properties of lightweight concrete. If Eq. (2) is satisfied, β_s may be taken as 0.75; and
- In accordance with Eq. (2), shear stress exceeding the current Code limit of $10\sqrt{f_c'}$ will be permitted for steeply inclined struts between load and reaction areas.

These updated provisions resolve the concerns and inconsistencies listed in the introduction. Additionally, the changes should lead to more economical design of deep footings and thick slabs because the beneficial effect of steep strut angles counteracts the size effect.

Acknowledgments

The experimental study described herein was funded by Florida International University. The authors wish to express their sincere gratitude for the university's support. The authors also gratefully acknowledge technical assistance and guidance from Joint ACI-ASCE Subcommittee 445-A, Shear & Torsion-Strut & Tie, and ACI Subcommittee 318-E, Section and Member Strength, as well as numerous ACI colleagues, including Jeff Rautenberg, Santiago Pujol, David Sanders, Dan Kuchma, Karl-Heinz Reineck, Evan Benz, and the late Mete A. Sözen.

References

1. ACI Committee 318, "Building Code Requirements for Structural Concrete (ACI 318-02) and Commentary (ACI 318R-02)," American Concrete Institute, Farmington Hills, MI, 2002, 443 pp.

2. Schlaich, J.; Schäfer, K.; and Jennewein, M., "Toward a Consistent Design of Structural Concrete," *PCI Journal*, V. 32, No. 3, May-June 1987, pp. 74-150.

3. ACI Committee 318, "Building Code Requirements for Structural Concrete (ACI 318-14) and Commentary (ACI 318R-14)," American Concrete Institute, Farmington Hills, MI, 2014, 519 pp.

4. Laughery, L., and Pujol, S., "Compressive Strength of Unreinforced Struts," *ACI Structural Journal*, V. 112, No. 5, Sept.-Oct. 2015, pp. 617-624.

5. Reineck, K.-H., and Todisco, L., "Database of Shear Tests for Non-Slender Reinforced Concrete Beams without Stirrups," *ACI Structural Journal*, V. 111, No. 6, Nov.-Dec. 2014, pp. 1363-1372.

6. Reineck, K.-H.; Bentz, E.C.; Fitik, B.; Kuchma, D.A.; and Bayrak, O., "ACI-DAfStb Database of Shear Tests on Slender Reinforced Concrete Beams without Stirrups," *ACI Structural Journal*, V. 110, No. 5, Sept.-Oct. 2013, pp. 867-875.

7. Rezaei, N.; Klein, G.; and Garber, D., "Struts Strength and Failure in Full-Scale Concrete Deep Beams," *ACI Structural Journal*, V. 116, No. 3, May-June 2019, DOI: 10.14359/51713306.

8. Van den Hoogen, M.G.M., "Beam or Truss Mechanism for Shear in Concrete: Problems Converting a Beam into a Truss," MSc. thesis, Department of Structural Engineering, Technical University Delft, Delft, the Netherlands, 2013, 128 pp.

9. Zsutty, T.C., "Shear Strength Prediction for Separate Categories of Simple Beams Tests," *ACI Journal Proceedings*, V. 68, No. 2, Feb. 1971, pp. 138-143.

10. Bazant, Z., and Kim, J.-K., "Size Effect in Shear Failure of Longitudinally Reinforced Beams," *ACI Structural Journal*, V. 85, No. 5, Sept.-Oct. 1984, pp. 456-468.

11. Belarbi, A.; Kuchma, D.A.; and Sanders, D.H., "Proposals for New One-Way Shear Equations for the 318 Building Code," *Concrete International*, V. 39, No. 9, Sept. 2017, pp. 29-32.

12. Klein, G.; Botros, A.; Andrews, B.; and Holloway, K., "Dapped Ends of Prestressed Concrete Thin-Stemmed Members: Part 2, Design," *PCI Journal*, V. 62, No. 2, Mar.-Apr. 2017, pp. 83-100.

Received and reviewed under Institute publication policies.

Gary J. Klein, FACI, is Executive Vice President and Senior Principal at Wiss, Janney, Elstner Associates, Northbrook, IL. His research interests include behavior and design of precast concrete elements and discontinuity regions. He is a licensed structural engineer specializing in failure investigation and a member of ACI Committee 318, Structural Concrete Building Code, and Joint ACI-ASCE Committee 445, Shear and Torsion. Klein received the 2010 ACI Wason Medal for Most Meritorious Paper and the 2016 ACI Charles S. Whitney Medal. He was also elected to the National Academy of Engineering.

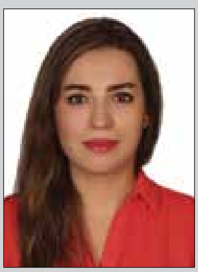

ACI member **Nazanin Rezaei** is a PhD candidate at Florida International University, Miami, FL. She was the head of the Structural Department at E-lood Consulting Engineers, Tehran, Iran, for 3 years. She is a member of Joint ACI-ASCE Committee 445, Shear and Torsion. She received her MS from Iran University of Science and Technology, Tehran, Iran.

ACI member **David Garber** is an Assistant Professor at Florida International University. His research interests include plasticity in structural concrete and behavior of prestressed concrete members. He is a member of ACI Committee 342, Evaluation of Concrete Bridges and Bridge Elements, and Joint ACI-ASCE Committees 423, Prestressed Concrete, and 445, Shear and Torsion. He received his BS from Johns Hopkins University, Baltimore, MD, and both his MS and PhD from The University of Texas at Austin, Austin, TX. He is a licensed engineer in Florida.

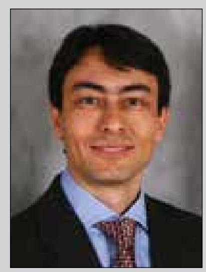

ACI member **A. Koray Tureyen** is Senior Associate at Wiss, Janney, Elstner Associates. He specializes in failure and damage investigations, structural and materials troubleshooting, and repair and rehabilitation. His research interests include shear, bond, and anchorage behavior of structural concrete. He is a member of ACI Committee 349, Concrete Nuclear Structures, and Joint ACI-ASCE Committees 408, Bond and Development of Steel Reinforcement, and 445, Shear and Torsion. He is a licensed engineer in Michigan.